AIP | Journal of Applied Physics

Frequency splitting of a multi-layered electric ring resonator

S. G. Kim, K. H. Kim, H. S. Jung, H. Cho, and E. M. Choi

Citation: J. Appl. Phys. **110**, 013105 (2011); doi: 10.1063/1.3605493

View online: http://dx.doi.org/10.1063/1.3605493

View Table of Contents: http://jap.aip.org/resource/1/JAPIAU/v110/i1

Published by the AIP Publishing LLC.

Frequency splitting of a multi-layered electric ring resonator

S. G. Kim,[1] K. H. Kim,[1] H. S. Jung,[2] H. Cho,[2,3] and E. M. Choi[1,2,a)]
[1]*School of Electrical and Computer Engineering, Ulsan National Institute of Science and Technology (UNIST), Ulsan 689-798, Republic of Korea*
[2]*Graduate School of Natural Sciences, Ulsan National Institute of Science and Technology (UNIST), Ulsan 689-798, Republic of Korea*
[3]*School of Nano-bioscience and Chemical Engineering, Ulsan National Institute of Science and Technology (UNIST), Ulsan 689-798, Republic of Korea*

(Received 7 April 2011; accepted 24 May 2011; published online 13 July 2011)

We present experimental results on the multilayering effects of an electric ring resonator. The electromagnetic response of the electric ring resonator is measured via a scattering matrix using a vector network analyzer at the X-band frequency. Structures of the electric ring resonator with up to four layers were tested and analyzed using commercial software. We demonstrate that, in an electric ring resonator, the electric and magnetic dipole polarization effect gives rise to resonance frequency splitting when the cell is multilayered. © *2011 American Institute of Physics*. [doi:10.1063/1.3605493]

I. INTRODUCTION

Metamaterial based on a split ring resonator (SRR) has been successfully tested, and real applications of the material have been carried out over a wide range of frequencies in the last few years.[1] Researchers have studied various SRR shapes for practical realization and better understanding of the structure.[2] The scalability of geometry for a wide frequency range is such that metamaterials are powerful devices for versatile applications.[3–5,8] Frequency selective behavior is a peculiar response of an SRR having periodic structure. This resonance behavior of the SRR from a few gigahertz to terahertz has drawn attention in terms of application to antennas, switches, filters, and absorbers, and the frequency range has been extended to the infrared regime recently.[3,6,7]

The first perfect metamaterial absorber realized by the combination of an electric ring resonator (ERR) and a cut wire was introduced by Landy *et al.*,[3] and studies on similar ERR structures followed.[9,10] Various perfect metamaterial absorbers using ERRs have since been reported.[9,10] The challenges are to realize a three-dimensional stacked metamaterial structure and to overcome the dependency of absorption on the incident electromagnetic wave angle. Extensive studies have been conducted to address these challenges for a single layer of a SRR structure.[11,12] However, the resonance and polarization behaviors of a multilayer metamaterial has not yet been investigated. In this study, we explore resonance and polarization behaviors of multilayer ERRs that were initially proposed in the first metamaterial absorber study.[3] The ERR consists of two regular SRR structure sharing a center wire that takes the role of an electric coupling with the external electromagnetic wave. A gap with a dielectric filling of each SRR provides the capacitance of the LC circuit, and the entire wire provides inductance, giving a resonance frequency to the LC circuit of the ERR unit cell.

This paper mainly focuses on the multilayer effect of the ERR structure by investigating a single layer of ERR unit-cell arrays. All experimental results are analyzed and compared using the commercial High Frequency Structure Simulator (HFSS, v12).

II. EXPERIMENT ON A MULTILAYERED ERR

In this study, we explore resonance and polarization behaviors of multilayer ERRs. The ERR structure in the experiment is shown in Fig. 1(c).[3] The fabricated planar array of ERR cells on a 200 mm × 200 mm FR4 substrate is 46 × 17 cells (i.e., a total of 782 cells), as shown in Figs. 1(a) and 1(b). Each cell has dimensions of $a_1 = a_2 = 3.9$, $t = 0.6$, $g = 0.606$, $w = 4.2$, and $h = 12$, in units of millimeters, as in Fig. 1(c). The thickness of the FR4 substrate is 0.6 mm. As shown in Fig. 2, the ERR is situated in between two quad-ridge horn antennas, and the scattering parameters (*S* parameters) are measured by an Agilent Vector Network Analyzer (PNA-X N5242 A, 10 MHz-26.5 GHz). As indicated in Fig. 2, the measurement was made under two different polarizations: the electric field being polarized in the *y* direction (hereafter denoted *y* pol) and the electric field being polarized in the *x* direction (hereafter denoted *x* pol). The direction of wave propagation is normal to the plane of the ERR layer (*z* direction). The multilayer measurement was made on up to four ERR layers by stacking identical single ERR layers one by one.

The electromagnetic response of the multilayer ERR was analyzed using HFSS, v12. A Floquet port option of the software enables the periodic ERR cell structure to be simulated considering only a single ERR cell. Figure 3 compares the experimental results of transmission data compared with simulation results. Slight redshifts in the frequency for both polarization conditions in the simulations with respect to experiments were found, which may be attributed to

a)Author to whom correspondence should be addressed. Electronic mail: emchoi@unist.ac.kr.

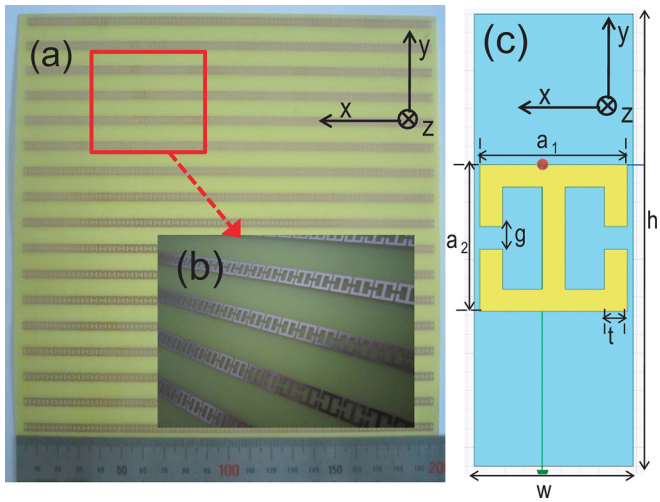

FIG. 1. (Color online) The planar array of ERR unit cells and experimental setup: (a) a picture of a single layer of ERR arrays, (b) a magnified portion of (a), and (c) the ERR unit cell.

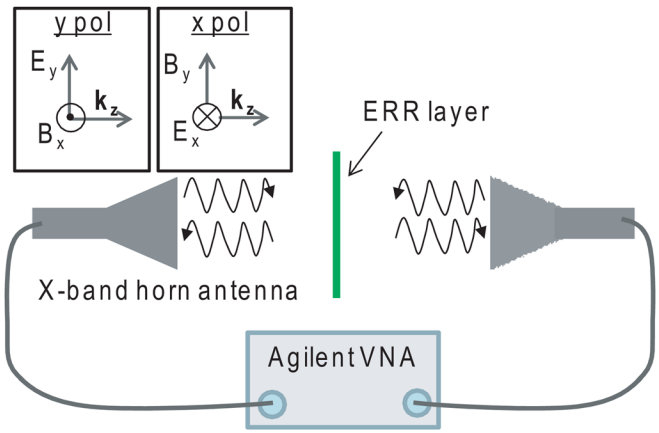

FIG. 2. (Color online) The experimental setup for a multilayer ERR test.

manufacturing imperfection. We measured the geometrical dimensions of a unit cell via optical microscopy. We systematically found that both a_1 and a_2 were 20 μm smaller than the designed values, and the thickness of ERR rods, t, was 30–60 μm smaller on average. This would result in a frequency redshift of $\sim$50 MHz in the HFSS simulation and thus explained the single-layer frequency shift. However, as the number of layers increases to 2, 3, and 4, not only manufacturing error but also alignment error may contribute, which partially explains the relatively large resonance frequency mismatches in multilayer tests. The transmission (S_{21} parameter) data have a Lorenzian distribution centered at the resonance frequency of the ERR cell in the single-layer and double-layer results for both y and x polarizations in both experiments and simulations. The behavior of resonance peaks under both polarization conditions and for all layers has qualitative agreement between experiments and simulations. Especially in the x pol case, the transmission data have an asymmetrically broad Gaussian distribution in both experiments and simulations. Notably, in the x pol case, another resonance peak is observed when the ERR is no longer a single layer, as predicted in simulations. The y pol case also shows two resonance peaks, both in the experiment and simulation when there are more than three layers, is greater than three (a very weak peak appears on the left of the curve in Figs. 3(c) and 3(g)). This implies two important findings. First, higher-order excitations start to appear when layers are stacked, which may deteriorate the functionality of the metamaterial absorber. Second, the resonance peaks are either blue-shifted or red-shifted when the higher-order excitation starts to appear, which may affect some frequency-specified applications.

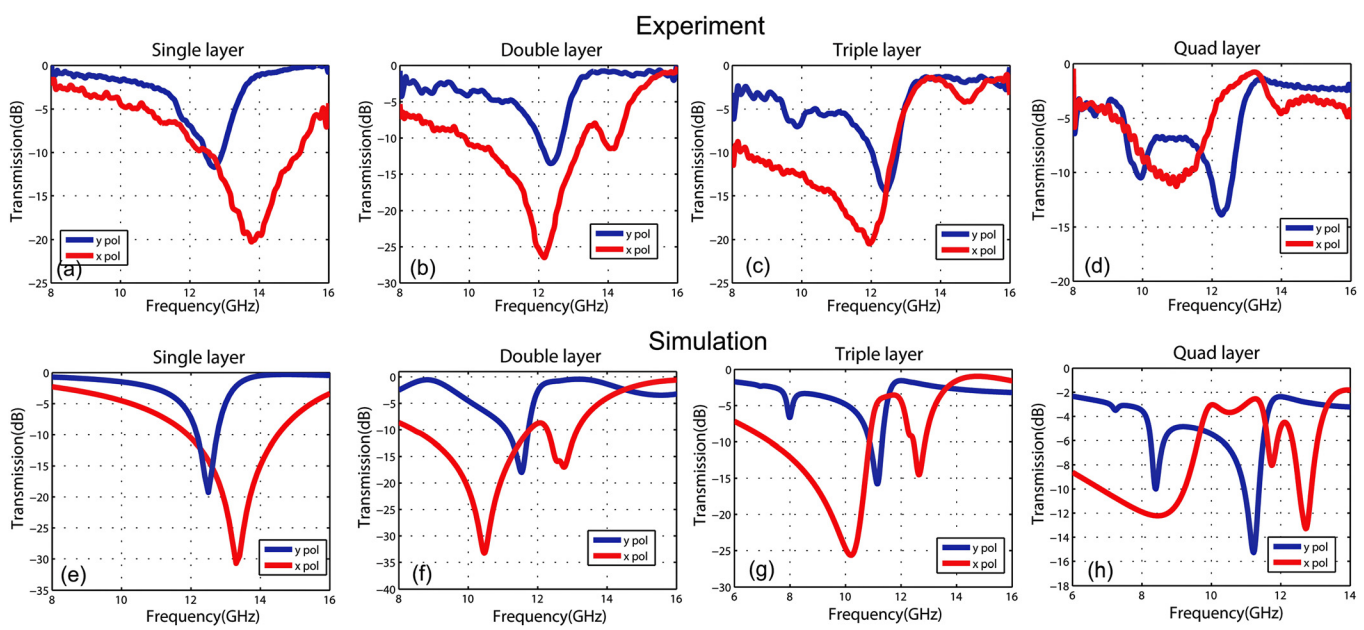

FIG. 3. (Color online) Experimental and simulation transmission spectral results of the multilayer ERR test, (a)–(d): Experimental results and (e)–(h): simulation results. A single-layer, double-layer, triple-layer, and quadruple-layer ERR were tested. Blue curves show the results for y pol (the electric field is polarized in the y direction), and red curves show the results for x pol (the electric field is polarized in the x direction).

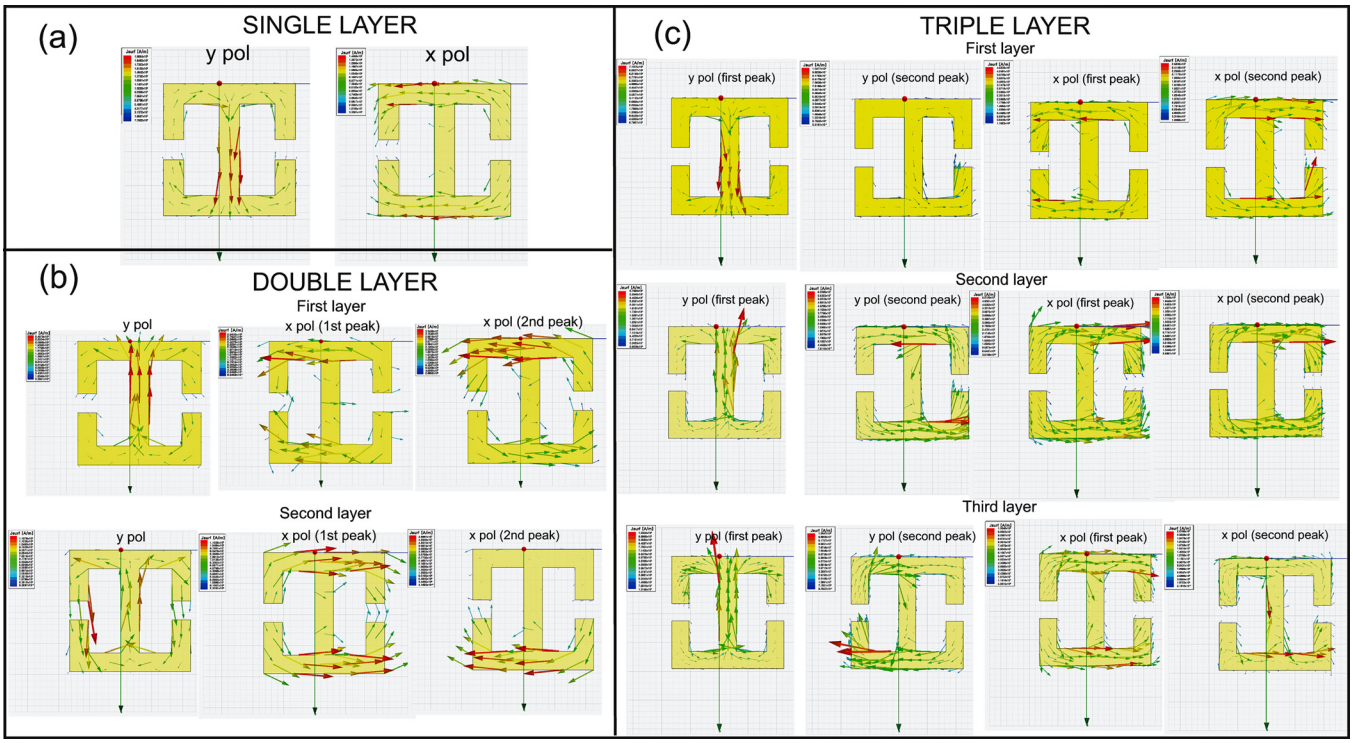

FIG. 4. (Color online) Simulation results for the surface current density of (a) a single-, (b) double-, and (c) triple-layer structure. For the double and triple layer structures, the surface current density in each layer is plotted for *x* pol and *y* pol. The first and second peaks are the lower-frequency peak and higher-frequency peak, respectively.

III. ANALYSIS OF RESULTS FOR A MULTILAYER ERR

Further investigations on the polarization show that the higher-order excitation is related to the surface current distribution on the ERR.

With respect to the center point of the ERR unit cell, *y* pol for the single-layer structure provides a symmetric current distribution, which can be expressed as $J_{s,A}(x, y) = J_{s,B}(-x, -y)$, where *A* and *B* represent the ERR half unit[11] (for antisymmetry, $J_{s,A}(x, y) = -J_{s,B}(-x, -y)$. Likewise, *x* pol for the single-layer structure provides a symmetric current distribution. The current distributions for the multilayered ERR are shown in Fig. 4 and summarized in Table I. For a single-layer, both *x* pol and *y* pol excite only the dominant surface current distribution owing to the presence of the external electric field, as shown in Fig. 4(a). In the single-layer case, therefore, there is only one resonance peak for both *x* pol and *y* pol. In the *y* pol case, the initial electric coupling between the incident electric field and the center wire of the first layer is dominant, and the induced surface current density is shown in Fig. 4(a). Therefore there is one strong electric resonance peak. As the number of ERR layers increases from one to more than one, multiple resonance peaks appear, as shown in Fig. 3(b) and 3(c). However, the strongest resonance peaks in the double-layer and the triple layer, which are on the lower frequency sides, retain their symmetric current density distributions, as shown in Fig. 4(b) and 4(c). Therefore, they are the main resonance LC peak of the single ERR layer. It is notable that, in the *x* pol case, there are two resonance peaks for multiple layers. The second resonance peak in the *x* pol case occurring at higher frequency but lower intensity than the first resonance peak for the double-layer structure has an antisymmetric surface current density distribution, as shown in Fig. 4(b). However, one should note that the second layer in the double-layer structure has an asymmetric surface current distribution in which there is no current flow at the top wire of the ERR ring, whereas there is current flow at the bottom wire of the ERR ring. In the *x* pol case for the triple-layer structure, the current density configuration is symmetric except for the third layer, which has an asymmetric current distribution similar to that of the second layer in the double-layer structure, and the center wire has current flow unlike that of the first and second layers in the triple-layer structure. This finding might be due to magnetic coupling between adjacent layers exciting higher-order resonance. For *x* pol, the electric coupling, initially attributed to the incident electric field of the incoming wave, in the short arms of the ERR (the top/

TABLE I. Summarized current distribution symmetry.

		1st peak		2nd peak	
		y pol	*x* pol	*y* pol	*x* pol
Single layer		symmetry	symmetry		
Double layer	1st layer	symmetry	symmetry		antisymmetry
	2nd layer	symmetry	symmetry		asymmetry
Triple layer	1st layer	symmetry	symmetry	antisymmetry	symmetry
	2nd layer	symmetry	symmetry	antisymmetry	symmetry
	3rd layer	symmetry	symmetry	antisymmetry	asymmetry

bottom arms in Fig. 1(c)) between layers is dominant, owing to the proximity to the adjacent layer. Therefore, *x* pol is prone to resonance frequency splitting (i.e., splitting of the original ERR LC resonance frequency and the capacitive coupling frequency). *y* pol also excites a second resonance of the ERR circuit, owing to magnetic coupling between the layers, when the incident electric field excites a higher-order current distribution configuration that is antisymmetric for the triple-layer structure, as shown in Fig. 4(c). One observes that the current density distribution of the second peak of the triple-layer structure in the *y* pol case is the combination currents circulating in each SRR ring. Therefore, the center wire of the ERR has no effective current flow, whereas the short arms with the gaps have circulating current flow. In this case, the magnetic dipole introduces an induced current via coupling between adjacent layers, which is the case where the term for magnetic coupling between layers overwhelms the term for ERR electric coupling. As seen in Fig. 4, the current density in the *y* pol case in the single-layer and double-layer structures are symmetric distribution, as stated in Table I.

IV. CONCLUSIONS

We verified that multilayers of arrays of ERR cells have coupling between adjacent layers capacitively and inductively, which excites spurious resonances. This resonance peak splitting is more dominant when the electric field is polarized in the short arms of the ERR (which we denoted *x* pol) while the wave is propagating perpendicularly to the ERR-layer plane. Detailed analysis of the frequency splitting effect showed that the fundamental resonance peak has a symmetric surface current density distribution, while higher-order excitations have antisymmetric and asymmetric current distributions.

ACKNOWLEDGMENTS

The authors wish to thank J. H. So and W. S. Lee at the Agency for Defense Development for the use of quadridge horn antennas in the study.

This work was supported by the Basic Science Research Program through the National Research Foundation of Korea (NRF) funded by the Ministry of Education, Science and Technology (Contract No. 2011-0006023) and by the National Research Foundation of Korea Grant funded by the Korea Government (No. 2010-0029434).

[1]A. K. Azad, A. J. Taylor, E. Smirnova, and J. O'Hara, Appl. Phys. Lett. **92**, 011119 (2008).
[2]N. I. Landy, C. M. Bingham, T. Tyler, N. Jokerst, D. R. Smith, and W. J. Smith, Phys. Rev. B **79**, 125104 (2009).
[3]N. I. Landy, S. Sajuyigbe, J. J. Mock, D. R. Smith, and W. J. Padilla, Phys. Rev. Lett. **100**, 207402 (2008).
[4]J. Li and J. Liu, Microwave Opt. Technol. Lett. **53**, 276 (2011).
[5]H. T. Chen, J. Zhou, F. O'Hara, F. Chen, A. Azad, and A. J. Taylor, Phys. Rev. Lett. **105**, 073901 (2010).
[6]I. Gil, J. Bonache, J. Garcia-Garcia, and F. Martin, IEEE Trans. Microwave Theory Tech. **54**, 2665 (2006).
[7]J. Ginn, D. Shelton, P. Krenz, B. Lail, and G. Boreman, Opt. Express **18**, 4557 (2010).
[8]N. H. Shen, M. Massaouti, M. Gokkavas, J. Manceau, E. Ozbay, M. Kafesaki, T. Koschny, S. Tzortzakis, and C. M. Soukoulis, Phys. Rev. Lett. **106**, 037403 (2011).
[9]Y. Cheng and H. Yang, J. Appl. Phys. **108**, 034906 (2010).
[10]X. Liu, T. Starr, A. Starr, and W. Padilla, Opt. Express **104**, 207403 (2010).
[11]J. Garcia-Garcia, F. Martic, J. D. Baena, R. Marques, and L. Kelinek, J. Appl. Phys. **98**, 033103 (2005).
[12]W. Padilla, A. J. Taylor, C. Highstrete, and M. Lee, Phys. Rev. Lett. **96**, 107401 (2006).